PCCP

PAPER

View Article Online
View Journal | View Issue

Cite this: *Phys. Chem. Chem. Phys.*, 2019, **21**, 18138

Deductive molecular mechanics of four-coordinated carbon allotropes†

Ilya V. Popov,[ab] Victor V. Slavin,[c] Andrei L. Tchougréeff *[abd] and Richard Dronskowski *[def]

Received 21st June 2019,
Accepted 2nd August 2019

DOI: 10.1039/c9cp03504d

rsc.li/pccp

Deductive molecular mechanics is applied to study the relative stability and mechanical properties of carbon allotropes containing isolated σ-bonds. Our approach demonstrates numerical accuracy comparable to that of density-functional theory, but achieved with dramatically lower computational costs. We also show how the relative stability of carbon allotropes may be explained from a chemical perspective using the concept of strain of bonds (or rings) in close analogy to theoretical organic chemistry. Besides that, the role of nonbonding electrostatic interactions as the key factor causing the differences in mechanical properties (in particular, hardness) of the allotropes is emphasized and discussed. The ADAMAS program developed on the basis of this study fairly reproduces spatial and electronic structure as well as mechanical properties of carbon allotropes.

Introduction

A large variety of unique physical and chemical properties of carbon-based materials has stimulated intensive studies of natural[1] and artificially prepared carbon allotropes,[2] and such studies are typically aiming at creating new materials or expanding the horizons of possible applications of the old ones. For searching of new crystalline phases of carbon, tentatively existing under high pressure, but metastable at standard conditions,[3] or for predicting the structures[4,5] of the phases, detected during the cold-phase transformation between diamond and graphite,[6] a variety of techniques[7–9] has been developed and applied. The number of phases found in those ways has already exceeded five hundred according to SACADA database.[10]

All searching methodologies require an electronic-structure calculator underneath, allowing to find an energetically feasible realization of a given allotrope topology (the basis of allotrope classification used in SACADA) by a crystalline structure in physical 3D space and to calculate mechanical properties of proposed allotropes. In most cases, plane-wave density-functional theory (DFT) involving PAW pseudopotentials,[11] the undisputed workhorse of computational materials design, are used. Despite all their recognized advantages such as high reliability of the resulting structures and energies and a large number of available program packages,[12,13] they also have some limitations to be mentioned. The well known issue of DFT, emphasized for instance in ref. 14, is that the resource requirements of DFT are quite burdensome in the case of large unit cells. This factor becomes crucial whenever numerous systems need to be screened, and that is exactly the perpetual case in searching for new crystalline structures. Although being much faster than wave-function-based methods, the relatively high numerical costs of DFT call for the development of alternative approaches, allowing one to optimize geometry and estimate relative energies of allotropes in a more efficient way.[14] There is a general trend in exploiting machine learning which still (and substantially) rely on DFT benchmarks. In the present work we consider carbon allotropes from a different perspective and present a new, specialized, quantum-mechanical, and highly efficient numerical tool for electronic-structure calculations of the aforementioned materials. This method is based on deductive molecular mechanics,[15,16] treating carbon allotropes from a chemical perspective, namely as systems featuring covalent bonds between hybridized atoms. This approach successfully applied to the C_2 molecule[17] and to analysis of relative stability of diamond and graphite (graphene)[18] is used in the present paper for modeling carbon allotropes with four-coordinated carbon atoms and, consequently, isolated σ-bonds only (see some characteristic examples in Fig. 1),

[a] *A.N. Frumkin Institute of Physical Chemistry and Electrochemistry of the Russian Academy of Science, Moscow, Russia*
[b] *Independent University of Moscow, Moscow, Russia*
[c] *B. Verkin Institute for Low Temperature Physics and Engineering of the National Academy of Sciences of Ukraine, Kharkov, Ukraine*
[d] *Chair of Solid State and Quantum Chemistry, RWTH Aachen University, 52056 Aachen, Germany. E-mail: andrei.tchougreeff@ac.rwth-aachen.de, drons@HAL9000.ac.rwth-aachen.de*
[e] *Jülich–Aachen Research Alliance, JARA-HPC, RWTH Aachen University, 52056 Aachen, Germany*
[f] *Hoffmann Institute of Advanced Materials, Shenzhen Polytechnic, 7098 Liuxian Blvd, Nanshan District, Shenzhen, China*

† Electronic supplementary information (ESI) available. See DOI: 10.1039/c9cp03504d

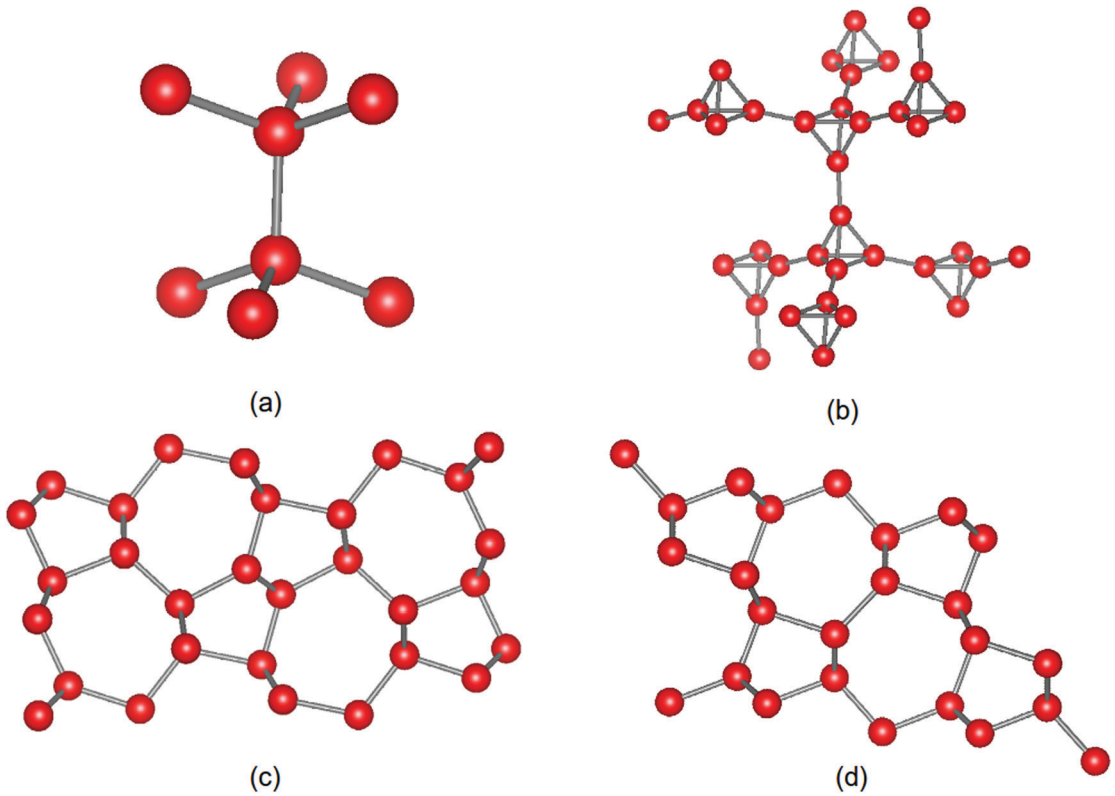

Fig. 1 Examples of allotropes with four-coordinated carbon atoms: **dia** – usual cubic diamond (a), **dia-a** – T-carbon (b) derives from diamond by replacing each C atom by a tetrahedral C_4 unit. This can be done not for all diamond C atoms but for every second, third *etc.* atom each proportion corresponding to a new allotrope. **cnw** – alias W-carbon (c) and **cbn** – alias M-carbon (d) are derived by replacing pairs of 6-membered rings by condensed 5- and 7-membered rings. The three-dimensional structures (c) and (d) are presented in the projection, allowing one to see the [5 + 7] recyclization. Similarly, not each pair of 6-membered rings, rather each second or third *etc.* may undergo recyclization, producing new allotropes or each second or third *etc.* layer of the 6-membered rings may undergo recyclization.

keeping allotropes featuring delocalized π-systems (and, thus, three- or even two-coordinated atoms) for future works. In this respect, the situation addressed here is simpler than in ref. 18. However, in variance with,[18] where the forms of the hybrids and the bond orders have been fixed by symmetry, in the present study either of these quantities is obtained by optimizing the total energies of allotropes (see below).

By looking at Fig. 1, one easily realizes that, despite its unprecedented completeness, the SACADA database can be never finished, since, *e.g.*, quadruply bonded carbon atoms in the diamond structure can be recursively replaced by tetrahedra formed by quadruples of such atoms featuring as well four external bonds in arbitrary depth and proportion (a kind of *Parkinson*[19] family of allotropes). Similarly, six-membered rings characteristic for diamond may undergo various types of recyclization yielding 5 + 7, 4 + 8 *etc.* condensed carbon cycles as well in arbitrary proportion every time yielding a new allotrope, so that, their number is, in fact, infinite.‡ Thus, besides numerical results on the energies and mechanical properties, an insight into the relative stability of allotropes and an analytic explanation for the trends in the calculated quantities is in demand. The chemical viewpoint applied in the present paper allows to consider carbon allotropes as ones built of condensed carbon cycles. From this point of view diamond is an infinite extension of adamantine,[20] while T-carbon[21] is that of tetrahedrane. Thus, as we shall show, even very old concepts such as strain applies with the necessary modifications also to carbon allotropes[22] and is able to provide an explanation of their relative stability, which can hopefully guide further research in this area.

Model

In what follows we apply our chemical approach based on bonds and hybridizations dubbed as deductive molecular mechanics (DMM).[15,16,23,24] Previously used in the carbon context to C_2[17] and to the pair of diamond/graphite.[18] It represents the total electronic wave function as a product of two-electron two-center wave functions of individual σ-bonds[25] formed by atomic hybrid orbitals (HOs) – combinations of s- and p-atomic orbitals (AOs) – as depicted in Fig. 2. Remarkably, this representation directly relates to the topological classification of allotropes[26] accepted in the SACADA database by identifying an "arc" in the

‡ Furthermore, the zeolite database[48] lists millions of the structures formed by vertex sharing tetrahedral SiO_4 units, which can be recast into respective four-coordinated carbon allotropes.[49]

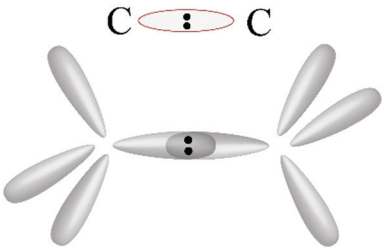

Fig. 2 Pictorial sketch of the two-electron bond wave function, characteristic for σ-bonded allotropes. The wave function of the entire crystal is an antisymmetrized product of similar functions referring to all bonds.

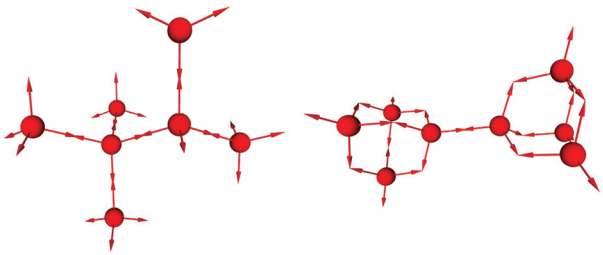

Fig. 3 The exact sp^3 hybrid orbitals yielding the energy minimum to the unstrained diamond structure (left) and the deformed hybrids sp^x (x = 1.5 for the bond between the C_4 units and x = 4.0 for those within the C_4 units) corresponding to the energy minimum for the strained T-carbon allotrope (b). Arrows represent the vector parts $\vec{v}$ of the sp^x hybrids pointing to the direction of the arrow.

topological representation with a corresponding σ-bond in the crystal. Within this setting the energy of a solid featuring solely σ-bonds arrives at:[18]

$$E = \sum_{\mathrm{A}} E_{\mathrm{A}} + \sum_{m} E_m + \frac{1}{2}\sum_{\mathrm{A}}\sum_{\mathrm{B}} E_{\mathrm{AB}}^{\mathrm{rep}} \qquad (1)$$

(A and B refer to arbitrary atoms in the crystal and m refers to the bonds present in the crystal). The "atomic" energies E_{A} are hybridization-dependent in general. Nonetheless, it was proven[18] that in the case of main-group IV atoms, E_{A} no longer depend on the hybridizations. Thus, the first sum in eqn (1) results in a constant "atomic" energy common for all allotropes, which does not affect their relative stability. By this, the number of meaningful contributions to the allotropes' energies reduces to only two. These are the "bond" electronic energies (BEE) E_m§ and the "repulsion" ($E_{\mathrm{AB}}^{\mathrm{rep}}$) energies. The latter cover the electrostatic interaction of charge distributions residing on atoms A and B.¶[17,18] The bond electronic energy of the m-th bond E_m was shown[17] to depend on two bonding indices, the Coulson bond order[27,28] P_m and the Mayer bond-order index B_m[29]

$$E_m = \frac{1}{2}(B_m \Delta_m - 4P_m t_m), \qquad (2)$$

where t_m is the one-electron hopping integral between the HOs forming the bond, and $\Delta_m = g_m - \gamma_m$ is the difference of one- and two-center electron–electron repulsion parameters.

The Coulomb atomic integrals are given by analytic expressions,[30] shown[18] to fairly reproduce the results of accurate DFT calculations on diamond, lonsdaleite (hexagonal diamond – **lon**) and graphene as regards to the relative position of these lowest-energy carbon allotropes on the energy scale and the experimental interatomic separations. The electronic problem for an individual (symmetric/homopolar) bond solves analytically[17] and P_m and B_m express through Δ_m and t_m so that the BEE for the m-th bond becomes:

$$E_m = \frac{1}{2}\left[\Delta_m - \sqrt{16t_m^2 + \Delta_m^2}\right]. \qquad (3)$$

§ Hence, E_m is not identical with the bond energy itself but rather only an electronic contribution to it.

¶ It is a combination of spherically symmetric quasi-Yukawa repulsion of charge distributions and of multipole interactions, absorbing all deviations from the spherical symmetry caused by hybridization.

The explicit account of hybridization of the AOs is another characteristic feature of the DMM approach. In it, each HO is a pair $(s, \vec{v})$ of a number s (the coefficient of the s-AO) and a triple of the coefficients of the p_x-, p_y-, and p_z-AOs incidentally transforming as a 3-vector $\vec{v}$ under the spatial rotations, which justifies the accepted notation. A convenient visualization of the systems of hybrids on each atom by hybridization tetrahedra (see Fig. 3) is thus possible. The expansion coefficients of HOs, residing on each carbon atom, over s- and p-AOs form orthogonal 4 × 4 matrices each containing 16 elements, which, due to orthonormality, are further reduced to six independent variables. These can be selected as, first, three angles, eventually forming a 3-vector $\vec{\omega}_{\mathrm{l}}$, describing the orientation of the set of the HOs as a whole. The shape of the hybridization tetrahedron is determined by the angles between the HOs. These six angles are uniquely determined by the four coefficients of s-AOs in the hybrids:[23]

$$\cos\theta_{mn} = -\frac{s_m}{\sqrt{1-s_m^2}}\frac{s_n}{\sqrt{1-s_n^2}}.$$

The weights of the s-AOs on each atom are subject to the normalization condition

$$\sum_{m=1}^{4} s_m^2 = 1, \qquad (4)$$

which leaves us with three independent variables for the shapes, which can also be selected as a 3-vector of angles $\vec{\omega}_{\mathrm{b}}$.

Eventually, the energy of a crystalline allotrope depends on atomic coordinates and hybridizations, which predetermine Δ_m and t_m in eqn (2) and (3). The quantities Δ_m and t_m are functions of the form and orientation of the HOs[23] expressed through the angles $\vec{\omega}_{\mathrm{l}}$; $\vec{\omega}_{\mathrm{b}}$ and of interatomic separations, so that finally the energy of an allotrope is a relatively simple function of the geometry variables and the angles $\vec{\omega}_{\mathrm{l}}$; $\vec{\omega}_{\mathrm{b}}$ for each atom in the unit cell. For example, the total energy of diamond reduces to:[18]

$$E_{\mathrm{D}} = -\frac{1}{2}(4t_{\mathrm{sp^3}} + \gamma) + E_{\mathrm{D}}^{\mathrm{rep}},$$

including the hopping integral (between the sp^3 hybrids forming the bond) dubbed $t_{\mathrm{sp^3}}$, the inter-atomic electron–electron repulsion dubbed γ and the sum of interatomic repulsion terms dubbed $E_{\mathrm{D}}^{\mathrm{rep}}$.

In addition, analytic expressions of gradients and Hessians with respect to these variables are available, so the minimum of the total energy including quantum-mechanical estimates of its electronic part are easily found by applying efficient optimization methods instead of tedious self-consistency procedures required within density-functional theory. Using the analytical energy Hessian we calculate the elasticity tensor c_{iklm} (see Appendix A) and, thus, the mechanical properties of the allotropes. The bulk and Young moduli are expressed in terms of c_{iklm}.

Results

Numerical results and computational efficiency

We implemented the DMM theory[15,16,23,24] sketched above in the computer package ADAMAS written with use of our in-house computational chemistry toolkit CARTESIUS_FORT[31] and performed calculations for carbon allotropes selected from the SACADA data base (13 allotropes). This selection satisfies two vague criteria: (i) it more or less uniformly covers the range of allotrope energies between the **dia** and **dia-a** (cubic diamond and T-carbon) allotropes; and (ii) contains in addition to the allotropes featuring unstrained six-membered rings (**dia**, **lon**) and the most strained three-membered ones (**dia-a**) also intermediate ones with 5 + 7 and 4 + 8 condensed rings. The full tables with optimized unit-cell parameters and calculated allotrope densities, relative energies and bulk moduli are given in the ESI.† The comparison of the ADAMAS results with the DFT-based data available in SACADA is presented graphically in Fig. 4 and 5. Using the parameter setting,[18] ADAMAS reaches a very good agreement: the absolute deviation from SACADA in the range 0–4 kJ mol^{-1} (it is slightly higher for the high-energy **lcs** and **dia-a** allotropes), eventually achieving chemical accuracy. The agreement is particularly good for the low-energy allotropes – those close to diamond and thus most prospective candidates for synthesis (for the **cfe**, **cfc** and **SiC12** allotropes, which can be characterized

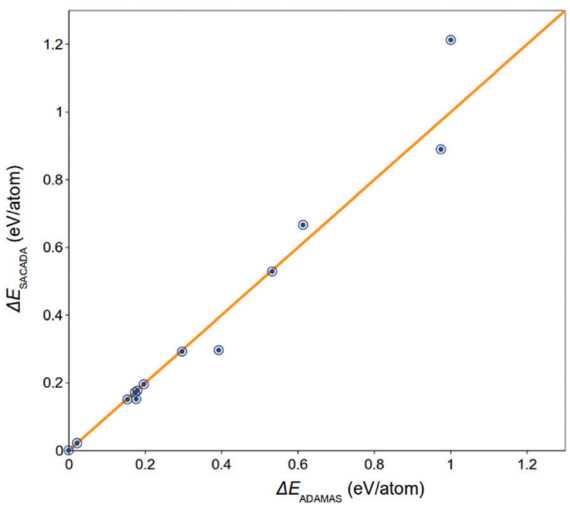

Fig. 4 Relative energies of allotropes relative to diamond calculated by the ADAMAS package as compared to the data available from SACADA data base.

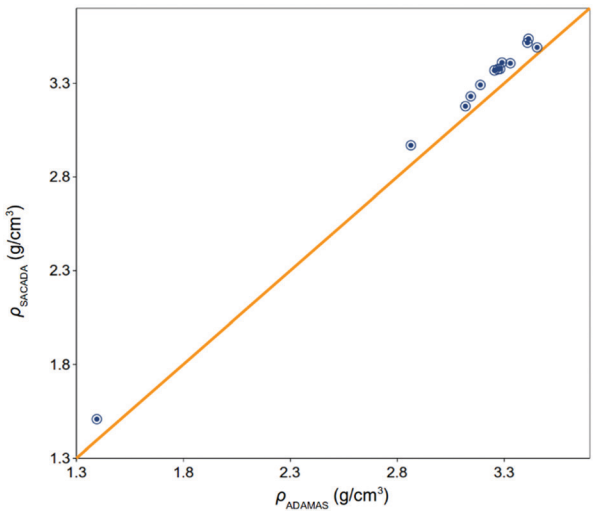

Fig. 5 Densities of allotropes relative to diamond calculated by the ADAMAS package as compared to the data available from SACADA data base.

as combinations of the **dia** and **lon**, the agreement is particularly spectacular: their energy relative to **dia** is on the scale of 1–1.5 kJ mol^{-1} according to SACADA; ADAMAS produces similar results – for details see ESI†). Provided, eventually infinite number of possible four coordinated allotropes, we assume that the selection made gives enough support to our approach on the level of a proof of a concept. The unit-cell parameters, obtained with ADAMAS, as well, demonstrate satisfactory agreement with the SACADA values (the mean relative deviation is 1.2%) although, shows slight underestimate. This level of accuracy is reached with incomparably smaller numerical effort: instead of days of calculations on mainframes by standard PAW-DFT solid-state packages (see *e.g.*, ref. 7–9 and 32), ADAMAS produces results of the same numerical quality within minutes on a notebook.‖

There are no available standard values of the allotropes' bulk moduli. Those given in SACADA may differ by 50–80 GPa for the same allotrope, depending on the calculation method. We discuss the elasticity issues below.

3.2. Relative stability of allotropes seen through the bond strain and hybridization

In view of the reached numerical agreement between SACADA's DFT-based energies and structures and those coming from our DMM procedure, let us analyse the possible sources of the energy differences between the carbon allotropes. The chemical analogy between carbon allotropes and polycyclic alkanes, as mentioned in the Introduction, suggests that the repulsion contribution E_{AB}^{rep} in eqn (1) causes the ring strain for the atoms falling in the eclipsed conformation. It is believed to be an

‖ Technically ADAMAS is easy to use. A user provides initial crystal structure in the POSCAR format of VASP[12] easily derivable from the *.cif files given *e.g.*, in SACADA with use of the tools amply available in the Internet. An additional file is required to specify the details of the calculation procedure. Exemplary input files are given in the Supplement. The package is available for usage through the Netlaboratory system[50] at https://netlab.cartesius.info

important factor of cycloalkanes (in)stability. Our calculations, however, show that the share of repulsion in the allotropes's total relative energies usually does not exceed 20% while its absolute value varies from 2 to 8 kJ mol^{-1}. The only exception is T-carbon where it contributes 35% to its relative energy above diamond, so that even in this case it is not the dominant source of thermodynamic instability of the most strained of the considered allotropes. Moreover, in several cases the relative total and relative repulsion energies have different signs. This is to say that the key factor affecting the relative stability of carbon allotropes is the difference of covalent bonding energies. We will now concentrate primarily on this contribution. To analyze covalent bonding one needs to have an adequate measure of it. The authors[32] used ICOHP (integrated crystal orbital Hamilton population, the contribution of a particular bond to the band-structure energy) as a suitable measure *a posteriori* extracted from the results of DFT calculations with use of the LOBSTER package.[33] Here we use directly the bond electronic energies (BEE) employed in the calculations as a measure of covalent bonding.

In Fig. 6 the BEEs for bonds in different allotropes are plotted against the bond lengths. The blue line corresponds to the BEE in diamond, formed by two ideal sp^3 hybrids aligned with the bond. As shown previously[18] and obvious from the Figure, the diamond BEE is almost linear for the chemical range of the bond lengths.

Fig. 6 also reveals that the points are quite scattered around the line: the bonds with equal lengths may have significantly different BEEs, either higher or lower than those,

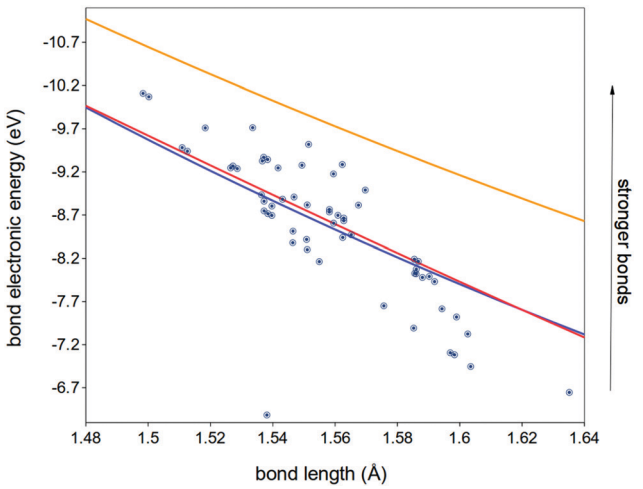

Fig. 6 Bond electronic energies (BEE) of the bonds in carbon allotropes plotted against their lengths. The red line corresponds to the bond, formed by ideal sp^3 HOs collinear to the bond. The blue line is an exponential approximation ($170.3\exp(-1.92d)$) for E_m analogous to the exponential approximation of ICOHP.[32] The mean absolute deviation of the exact BEEs from the red line is 0.46 eV and the mean relative deviation is 6.1%. For the exponential fit the mean absolute deviation is 0.47 eV and the mean relative deviation is 6.2%. The orange line is the ICOHP distance dependence.[32] Remarkably, it is almost ideally parallel to the BEE lines indicating the close analogy between the *a posteriori* covalence measure ICOHP and its direct measure: BEE.

Fig. 7 Schematic representation of vector parts of HOs, forming a (strained) bond between the left-end (L) and right-end (R) atoms of this bond.

corresponding to the diamond BEE at each given distance. This is in a line with the latest analysis[32] showing a similar scattering of the LOBSTER[33] derived ICOHP covalence measure *vs* bond lengths. In order to analyze this behavior we notice that the BEEs from eqn (2) or (3) depend on the composition of the constituent HOs and on their directions relative to the bond lines. Specifically, the hopping integral between the HOs of the bond is:[23]

$$t = t_{ss}s_L s_R + t_{sp}\left(s_L\sqrt{1-s_R^2}\cos\chi_R + s_R\sqrt{1-s_L^2}\cos\chi_L\right) + \sqrt{1-s_L^2}\sqrt{1-s_R^2}\left[t_{pp\pi}\sin\chi_L\sin\chi_R + t_{pp\sigma}\cos\chi_L\cos\chi_R\right], \quad (5)$$

(subscripts L and R refer to the "left" and "right" ends of the bond and the bond index m is omitted here for brevity). The angles are defined in Fig. 7. For the AO–AO hopping integrals in eqn (5) the usual approximation $t_{\mu\nu} = t^0_{\mu\nu}S_{\mu\nu}$ is used where $S_{\mu\nu}$ is the overlap integral between atomic orbitals μ and ν.

Reiterating, we notice that the theory dubbed deductive molecular mechanics is not only numerically efficient but also allows one to analyze the numerical results in fairly qualitative geometrical terms. An example of such reasoning goes as follows. In four-coordinated allotropes each carbon atom has four nearest-neighbors and thus its coordination tetrahedron is defined by four interatomic separations and four unit vectors $\vec{e}_m$ pointing to the neighbors. It is easy to figure out[24] that the number of variables describing the projections of four neighbor atoms on a "celestial sphere" drawn around the central one equals to eight (declination and ascension angles for each of the neighbors). Three angles are required to describe the orientation of the entire coordination tetrahedron (the set of four nearest neighbors) relative to laboratory frame, so that five variables remain for its shape. That large number of degrees of freedom makes the coordination tetrahedra in allotropes *a priori* quite flexible. By contrast, hybridization tetrahedra possess much more restricted flexibility: they are fully parameterized each by six angles collected in two 3-vectors $\vec{\omega}_l$; $\vec{\omega}_b$ of which the first is reserved for the orientation of the hybridization tetrahedron as a whole, so that only three angular variables in $\vec{\omega}_b$ stay available for description of its shape. Pragmatically, it means that the angles between the HOs, for example, cannot get smaller than 90°, although the valence angles for sure can (*viz.* T-carbon). Another observation is that a plane accommodating two arbitrary HOs of a given atom must be orthogonal to that accommodating two remaining HOs[34]

although the valence angles at a central atom as well as those between the planes formed by the central atom and disjoint pairs of its neighbors may take any value. The lack of the flexibility of the hybridization tetrahedra relative to the coordination ones may lead to misfits between the directions of the bonds (vectors $\vec{e}_m$) and the directions of the HOs (vectors $\vec{v}_m$). This serves as a source of energy excess (strain) in the allotropes where respective misfits occur. These misfits and their energy effect may be quantified by the angles χ_R, χ_L (Fig. 7). Assuming for the moment that the hybridization tetrahedra maintain their ideal sp^3 shape (thus, $s_L = s_R = \frac{1}{2}$) and inserting the expansions of cosines for small χ_{Rm}, χ_{Lm} in eqn (5), we conclude that the sum of electronic strain energies of the bonds (excess over the diamond structure) of an allotrope is

$$\delta E_s = K_s \sum_m \left({\chi_{Rm}}^2 + {\chi_{Lm}}^2 - 2k\chi_{Rm}\chi_{Lm} \right) \qquad (6)$$

with a (positive) coefficient K_s coming from eqn (3) and (4) as a combination of hopping integrals and bond orders (for more details see Appendix B). Since $k < 1$, the above quadratic form is positively definite, thus the bond strain leads uniquely to the energy increase as compared to the ideal (diamond) structure. In the range of realistic bond lengths k stays almost constant, thus for further estimates we use its transferable value ≈ 0.3. This finding suits for an analysis of the numerical data tentatively yielding a simple model of BEE. In Fig. 8 we plot the BEEs as calculated against the corresponding bond lengths and strain parameters:

$${\chi_m}^2 = {\chi_{Rm}}^2 + {\chi_{Lm}}^2 - 2k\chi_{Rm}\chi_{Lm}$$

Although there is still a considerable scattering, even with such a simple model we achieved a better representation of the BEEs as compared to one dependent on the interatomic separation only (Fig. 6). The mean absolute deviation reduces to 0.41 eV and the mean relative deviation down to 5.5% (in ref. 32 the mean absolute deviation of the ICOHP values from the exponential fit amounts 0.71 eV). However, the deviations are still significant. Moreover, we see that some numerical points fall below the fitting surface, which cannot be explained by the model with the strictly sp^3 hybridization tetrahedra (the energy correction eqn (6) is positive definite). The agreement improves if one recollects that within the numerical calculation the deformation of hybridization tetrahedra that is the variation of the coefficients of the s-AOs and thus changing the shapes of hybridization tetrahedra was allowed.

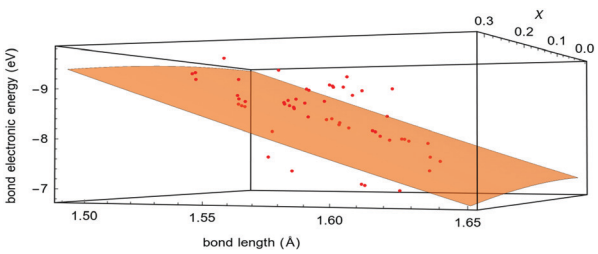

Fig. 8 Bond electronic energies as the function of bond length and bond strain measure χ.

This yields further energy corrections affecting BEEs. Allowing, along with the bond strain also small variations of the s-weights around their ideal sp^3 value of $\frac{1}{2}$, permits to accurately reproduce the exact BEE: the mean relative deviation is then equal to 1.12% and the mean absolute deviation is 0.10 eV. This is by an order of magnitude smaller than in the model with rigid hybridization tetrahedra or in those relying solely upon the bond lengths.

It is of interest to understand where the increase of the BEE on account of the variation of s's could come from and to trace the consequences of this for the overall energetics of the allotropes. We notice that for a symmetric bond with collinear HOs the maximum of the hopping integral corresponds to the value of the s-coefficients of *ca.* 0.77 (see Fig. 9), which is fairly larger than in the ideal sp^3 hybrids ($\frac{1}{2}$). Thus, an increase of s increases the BEE of the corresponding bond and the bond energy as well. This is precisely what happens in T-carbon. Here the HOs in the unstrained C–C bonds between the C_4 units feature much higher s-AOs' contribution ($s \approx 0.65$) than those in the highly strained (the maximal value of χ among of all bonds: 30.6°) C–C bonds within the C_4 units ($s \approx 0.44$).

These findings are parallel to the analysis[35] based on the LOBSTER covalence measure ICOHP. The BEE covalence measure (parallel to ICOHP) is as well larger for the C_4–C_4 bond than that for the C–C bond in diamond (and, of course, than that for the C–C bond within C_4 units). The analysis[35] also indicates the importance of the s-states in the formation of the C_4–C_4 bonds.

The discovery of allotropes with the BEEs (ICOHPs) larger than in diamond sparkles hopes on finding carbons more stable than the latter (see ref. 36 where more stable allotropes featuring a combination of three and four coordinated atoms had been proposed). Even in T-carbon the gain in BEE for the unstrained C_4–C_4 bond is that large that despite stronger repulsion (due to smaller bond length) the bond energy any way remains larger than in diamond. However, there are purely geometrical arguments proving that the hopes to find more stable exclusively four coordinated allotropes may be unfounded.

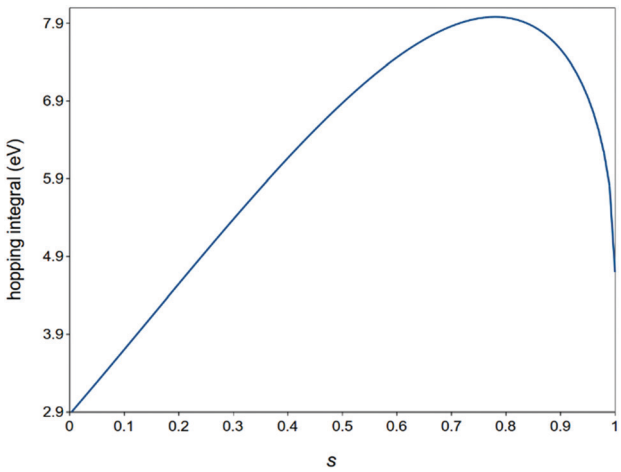

Fig. 9 Hopping integral as a function of s-contribution for a symmetric 1.544 Å C–C bond whose hybrids are pointing along the bond.

Indeed, due to the normalization condition eqn (4), the variations of the *s*-amplitudes δs_m's cannot be simultaneously negative or positive for all bonds incident to a given atom (for all its HOs).** Thus, the BEE's gain acquired through adjustment of the shape of the hybridization tetrahedron to the direction of one or more incident bonds is mandatory compensated by losses in other bonds (see formal proof in Appendix C).

In ref. 18 we observed the same effect for the pair of naturally occurring carbon allotropes: diamond and graphene. In the latter, the BEE of its σ-bonds between sp^2 hybrids is larger than for the σ-bonds in diamond formed by sp^3 hybrids due to larger amplitudes of s-orbitals.

Since the BEE corrections linear in δs_m's vanish, the second order ones as coming from small rotations and deformations of the hybridization tetrahedra become important. The exact expression for the latter are known.[23] In Appendix D it is shown to be positive definite. Thus, the general conclusion is that despite eventually strong gains in covalent interactions (BEE's) of individual bonds the overall effect of small rotations and deformations of the hybridization tetrahedra is the increase of the total energy relative to diamond. Combination of these two explains why for the time being the only known allotrope candidating for a lower energy than diamond[32] features quite extended fragments formed by the sp^2 rather sp^3 hybridized carbon atoms (graphene "belts"). The allotropes formed by exclusively sp^3 hybridized carbon atoms including those recently found[14] with use of thoroughly trained neural network systematically have larger energy than diamond in agreement with our analysis.

In the present work, the quantities χ and δs serve as measures of the angular strain of the bonds and the strain of hybridization tetrahedra, respectively. In the literature, one can find other strain measures. For example, mean squared deviation of valence angles from ideally tetrahedral ones is introduced.[37] It has been shown to be useful for orientation because of a linear correlation (demonstrated, however, on a very limited material of allotropes derived by fractional replacement of carbon atoms in the diamond or lonsdaleite structures by the tetrahedral C_4 units) with both the total energy per atom going from diamond to T-carbon, and the bulk modulus (see below). Drawing an analogous graph for the allotropes addressed in the present paper (Fig. 10) shows rather different behavior: all allotropes except T-carbon fairly lie on a straight line having nothing to do with one tentatively joining diamond and T-carbon. That is to say that for different selections of allotropes the dependence of their energy on the average angular deformation[37] considerably differs. By contrast, using the strain measures χ and δs allowed us to fairly fit the BEEs at least in the selected variety of allotropes.

A remarkable deviation form the situations covered by the strain measures is represented by the lowest energy **dia**/**lon** polytypes (**cfe**, **cfc**, **SiC12**). They feature ideal tetrahedral coordination so that their hybridization tetrahedra are not angularly distorted

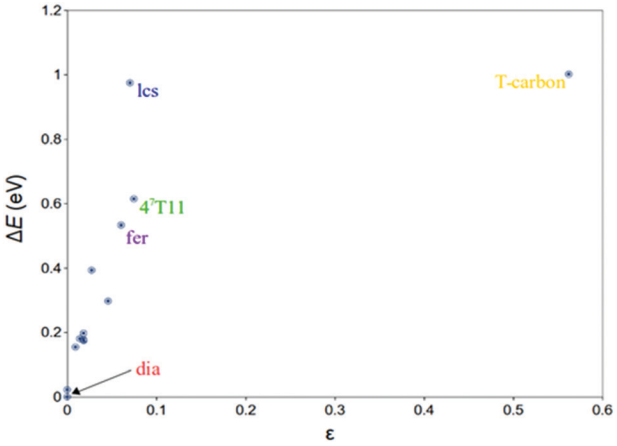

Fig. 10 Allotropes' energies relative to that of diamond plotted against the angular strain measure.[37]

and the deviations of the hybrids' directions from the bonds are negligibly small. In the absence of angular deformations, the structure variations in these polytypes reduce to the elongation/contraction of the C–C bonds. The bonding and nonbonding interactions contribute almost equally to the total relative energy. Neither ADAMAS nor SACADA show definite relation between the average bond lengths indirectly measured by the polytope density and its energy. The energies of all mentioned polytopes are squeezed between that of **dia** and **lon**, which is not the case of their densities of which **cfc** and **SiC12** are denser than diamond (have on average shorter bonds) and **cfe** has lower density (on the average bonds are longer). Accordingly, in two former polytypes the BEE is larger by absolute value than in diamond. Nevertheless, they are less stable (by 1.1 kJ mol^{-1}) because of the core repulsion increasing with density. Within the same setting in the **cfe** polytope featuring longer bonds the absolute value of BEE is smaller than in diamond partially compensated by the decrease of the repulsion energy, finally yielding the overall destabilization on the same scale relative to diamond.

3.3 Mechanical properties: the role of repulsion terms

As said before, ADAMAS allows for the calculations of the elastic properties of the allotropes. The numerical results are given in the ESI.† In general, the numerical values of the bulk moduli fit fairly well into the ranges obtained by different calculation methods. We note that as regards the experimentally accessible allotrope (diamond) the different numerical methods show a considerable scatter of 80 GPa (about 20%). In contrast, diamond's experimental bulk modulus is about 440 GPa[38] to be compared with our estimate of 453 GPa. Otherwise, the relative position on the hardness (habitually, understood as the value of the bulk modulus) scale produced by the ADAMAS package in the series of calculated allotropes follows the trends represented in the SACADA database (see Fig. 11 and Table S2, ESI†).

In order to find out what structural and electronic features might affect the allotropes' relative hardness we plot relative bulk moduli against the quantities describing these features (Fig. 12): the angular strain measure,[37] as well as with hybridization

** Remarkably, the amount of increase of *s* in the C_4–C_4 bond is almost equal to the total of decreases of *s*'s in the intra C_4 C–C bonds incident to the same atom.

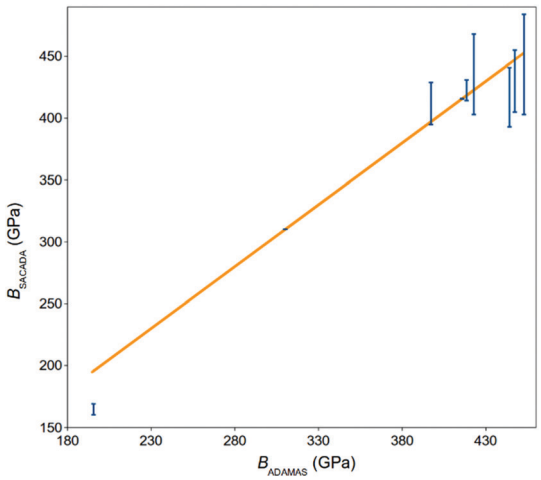

Fig. 11 Bulk moduli for a selection of carbon allotropes calculated by the ADAMAS package as compared to the data available in SACADA data base.

and bond strain measures (δs and χ). In either case there is no definitive correlation between whatever strain measure and the bulk modulus. In all cases, say, the **lcs** allotrope (ice II structure), featuring quite a considerable strain, but almost the same bulk modulus as diamond, falls out from all. On the other hand, T-carbon in all cases shows a significant reduction of the bulk modulus as compared to diamond.[21] Remarkably, either of the strain δs and χ manifest two branches: one linear, going from diamond to T-carbon, and a curved one, landing in **lcs** allotrope. The only observation, which we could derive so far is that the allotropes in the curved branches all feature 8-membered rings. This fact will probably find its explanation within the general theory of elastic properties of carbon allotropes yet to be developed.

Some general remarks can be given already now. In the literature, it is conjectured that the exceptional hardness (high bulk modulus) of diamond is caused by strong covalent bonding. To the best of our knowledge there have been no quantitative estimates of the role played by covalent bonding when it comes to mechanical properties. Since the DMM provides a clear-cut separation of covalent bonding (understood as BEE's) and repulsion contributions to the energy, we analyzed the relative values of their second derivatives with respect to atomic coordinates.

It turns out that the BEE's second derivatives are very small as compared to those of the repulsion contributions. As seen from Fig. 4, the dependence of the BEE on the bond length is pretty close to linear for the ''chemical'' range of interatomic distances actually covered by all allotropes (the same feature is observed in ref. 18). This translates into the BEE contribution to the second derivative of the total energy of less than 5%. This suggests that the key factor leading to the observed hardness of carbon allotropes is the repulsion between atomic charge distributions represented by the relatively short-range (quasi-)Yukawa terms, which tentatively explains the absence of reasonable correlation between the covalence-related strain measures and the bulk moduli.

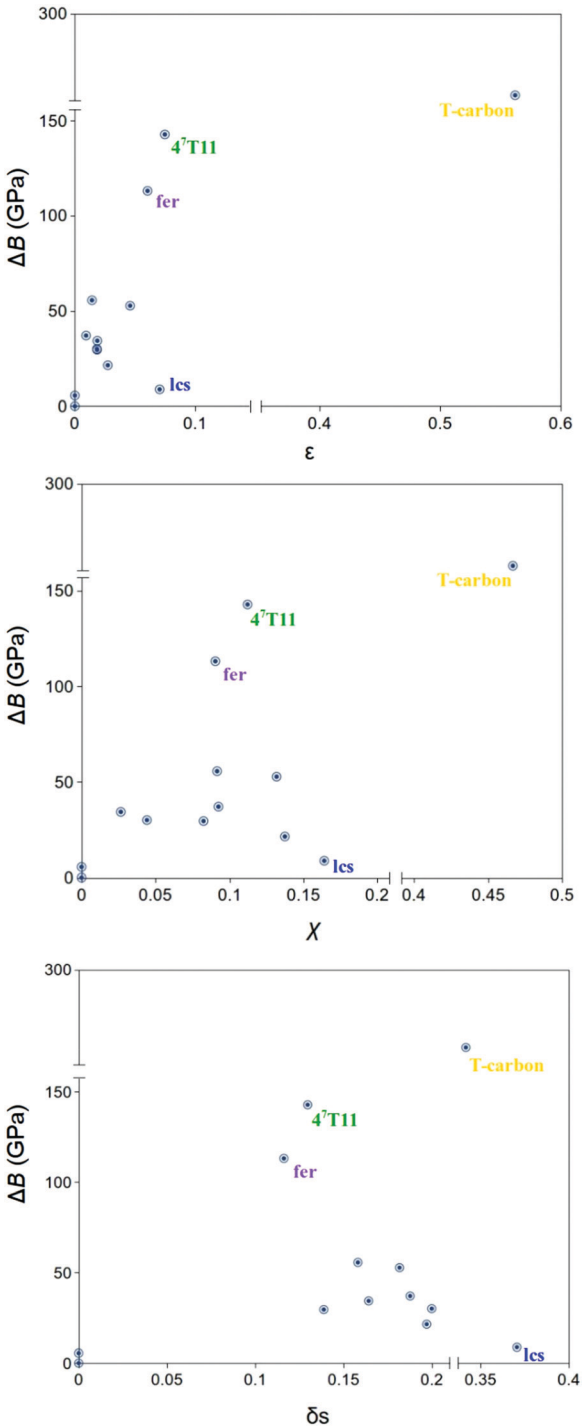

Fig. 12 Relative bulk moduli against mean square deviation of valence angles from valence angle in ideal tetrahedra (diamond) – above, against the bond strain measure χ – middle, and against mean square deviation of the s-amplitudes of HOs from the ideal sp^3 hybrides – bottom.

Conclusions

On the basis of the DMM which assures the chemical perspective of the carbon allotropes (one based on bonds and hybrids) we developed a new computer program ADAMAS. It is targeted at highly efficient electronic-structure calculations of carbon

allotropes. In variance with other solid states methods even those using semi-empirical parametrizations, which are all built upon the delocalized (Bloch) states or plane waves, our approach uses local description of the electronic structure: two-center bonds characteristic for the valence bond approximation[39] and hybrid orbitals. The latter allowed us to quantitatively address the strain of carbon–carbon bonds although proposed yet in ref. 40 but used directly for (electronic structure) calculation only now. In variance with the existing empirical quantum-mechanics based force fields[41–43] and their descendants we (i) use exact quantum chemical expressions for the parameters of electronic structure: bond orders and bond order indices (P_m and B_m, respectively) and (ii) determine forms and directions of the hybrids from the energy minimum condition: both are original features of our approach. This led us to the exact quantum mechanical expression for the allotrope energy, which turned out to be extremely efficient and precise.

In the present paper we tested the ADAMAS package on a selection of carbon allotropes containing 4-coordinated atoms. ADAMAS demonstrates more than a reasonable numerical accuracy in geometries, relative energies and mechanical properties as compared to the DFT-based methods reproducing their results within a chemical precision, but with by two orders of magnitude smaller requirements to computational resources in terms of both time and memory. The numeric results show that all directly considered four-coordinated allotropes have a higher energy than diamond. This happens despite the fact that in some of them certain fractions of C–C bonds are even stronger than those in diamond. Nevertheless, such local gains are compensated by unfavorable energy contributions from other bonds because of a limited flexibility of the hybridization tetrahedra.

The developed energy model also allows for estimates of mechanical properties, which are frequently missing in the SACADA database. For those allotropes for which the elasticity data are available in the SACADA database our estimates fall in the ranges of the values given there. For the rest they contribute the missing data.

Finally, despite different ''topology'' of four-coordinated allotropes, their bonds are characterized purely locally, by the strain measure χ. Similarly, each atom characterizes by the deviation of its hybridization tetrahedron from the ideal sp^3 shape. These characteristics (unlike the ''topology'' itself) directly translate to the relative energy of an allotrope relative to diamond. At the same time, the chemical DMM setting allows us to relate directly the allotrope's ''topology'' to its electronic wave function and its specific energy function, a feature unavailable in the solid-state physics-based approaches. By this, we arrived to an extremely efficient numerical tool providing to the workers in the field an easy access to the structure, energy and mechanical properties of carbon allotropes.

Conflicts of interest

There are no conflicts to declare.

Theoretical appendix

A. Hessian and elastic properties

The second derivatives of energy (Hessian matrix) were calculated analytically:

$$\eta_{ik}^{\mathrm{AB}}(\vec{r}) = \frac{\partial^2 E^{\mathrm{AB}}(\vec{r})}{\partial r_i^{\mathrm{A}} \partial r_k^{\mathrm{B}}}. \tag{A1}$$

Here A and B enumerate atoms, $E^{\mathrm{AB}}(\vec{r})$ is the energy of interaction of arbitrary atoms A and B, including the bond electronic energy (BEE) E_m from eqn (2) and (3), provided atoms are bonded, and the repulsion energy $E_{\mathrm{AB}}^{\mathrm{rep}}$. Vector $\vec{r} = \vec{r}^{\mathrm{A}} - \vec{r}^{\mathrm{B}}$ and r_i, r_k are Cartesian components of $\vec{r}$, i, $k = x, y, z$. The elasticity tensor reads:[44]

$$c_{iklm} = \frac{1}{V_0}\left\{ \sum_{\mathrm{AB}} \sum_{\{\vec{r}\}} \eta_{ik}^{\mathrm{AB}}(\vec{r}) r_l r_m + \frac{1}{2} \sum_{\mathrm{AB},jn} \left(\gamma_{ijl}^{\mathrm{A}} \gamma_{knm}^{\mathrm{B}} + \gamma_{ijm}^{\mathrm{A}} \gamma_{knl}^{\mathrm{B}} \right) M_{jn}^{\mathrm{AB}} \right\}$$

$$\gamma_{ikl}^{\mathrm{A}} = \sum_{\mathrm{B}} \sum_{\{\vec{r}\}} \eta_{ik}^{\mathrm{AB}}(\vec{r}) r_l, \tag{A2}$$

where V_0 is the unit cell volume, vector $\vec{r}$ runs through all pairs of interacting atoms. Due to the short range nature of the BEE and the exponential decay of the repulsion energy the summation in eqn (A2) converges rapidly. The quantities M_{jn}^{AB} are elements of the inverse matrix $\left(-\sum_{\{\vec{r}\}} \eta(\vec{r}) \right)^{-1}$. The first term in eqn (A2) has the regular form of elasticity theory. The second one is non-zero for the crystals without center of inversion only ($\gamma_{ikl}^{\mathrm{A}} = 0$ for the crystals with center of inversion). It takes care about adjustment of positions of atoms within unit cells in response to deformation of the latter.

The elasticity characteristics (Young modulus, bulk modulus, *etc.*) are expressed in terms of compliance tensor $s = c^{-1}$; *e.g.*, the anisotropic Young modulus $E(\vec{n})$ in the direction of a unit vector $\vec{n}$ is:[45]

$$E(\vec{n})^{-1} = n_i n_j s_{ijkl} n_k n_l \tag{A3}$$

and the bulk modulus K is:

$$K^{-1} = s_{iikk}. \tag{A4}$$

also known as Reuss average. In either formula the summation is understood over the repeating subscripts. According to ref. 46, eqn (A4) is the only rotation invariant of the compliance tensor of the relevant power.

B. Estimate of the parameters in eqn (6)

The coefficient K_s entering eqn (6) occurs after expanding trigonometric functions of eqn (5) due to small angles and multiplying hopping integral by minus quadruple bond order P_m. It yields the following expression:

$$K_s = \frac{\sqrt{3}}{2} P_m \left(t_{sp} - \sqrt{3} t_{pp\sigma} \right) = \frac{\sqrt{3}}{4} \left(t_{sp} - \sqrt{3} t_{pp\sigma} \right). \tag{B1}$$

The dimensionless parameter k reads

$$k = \frac{\sqrt{3}t_{pp\pi}}{t_{sp} - \sqrt{3}t_{pp\sigma}} \quad \text{(B2)}$$

and in the relevant range of bond lengths it stays almost constant (≈ 0.3 for bond length in diamond). If the bond length changes by 0.1 Å, coefficient k changes only by 0.02, which can be neglected.

C. Linear correction to the bond electronic energy due to variation of *s*-amplitudes

Due to normalization condition eqn (4) the variation of the *s*-amplitude of the m-th HO reads:[23]

$$\delta s_m = -(\delta\vec{\omega}_b, \vec{v}_m) \quad \text{(C1)}$$

where $\delta\vec{\omega}_b$ is the small variation of the triple of angular parameters responsible for the shape of hybridization tetrahedron on a given atom and $\vec{v}_m$ is the vector part of the m-th HO. Four vector parts of the four HOs in the ideal sp^3 hybrid sum to zero and thus the same is true for the sum of the first order corrections to the *s*-amplitudes:

$$\sum_{m=1}^{4} \vec{v}_m = 0 \Rightarrow \sum_{m=1}^{4} \delta s_m = 0 \quad \text{(C2)}$$

for each atom. Thus δs_m's cannot be simultaneously negative or positive (whichever leads to the energy gain) for all bonds incident to the given atom (respectively, for all its HOs) and actually sum to zero. Furthermore, the energy multipliers (whatever they are) at δs_m's in the expression for the correction to the energy linear in δs_m's are equal for equivalent bonds in diamond. Thus, the total of the corrections coming from the bonds incident to a given atom is proportional to the sum of δs_m's and thus vanishes. Thus, the BEE's gains linear in δs_m's or $\delta\vec{\omega}_b$ acquired through adjustment of the shape of the hybridization tetrahedron to the direction of one or more individual incident bonds are mandatory compensated by the losses in other bonds.

D. Second order energy corrections due to adjustment of shapes and orientations of hybridization tetrahedra

The second order corrections to the bond electronic energies coming from the small rotations and deformations of the hybridization tetrahedra had been derived yet in ref. 23. They are quadratic forms of the small variations $\delta\vec{\omega}_{bL}$, $\delta\vec{\omega}_{bR}$, $\delta\vec{\omega}_{lL}$, $\delta\vec{\omega}_{lR}$ (put in this order, see below) of the angular variables $\vec{\omega}_l$; $\vec{\omega}_b$ for hybridization tetrahedra residing on both ends of the bond. Each bond contributes terms proportional to the scalar squares of $\delta\vec{\omega}_{lT}$; $\delta\vec{\omega}_{bT}$ and the cross-terms coupling the rotations and deformations occurring on the left and the right ends of the bonds. Although in the individual bonds the rotations and deformations on the left and right ends are coupled (the cross-terms $\delta\vec{\omega}_{lR}$, $\delta\vec{\omega}_{bR}$ are present), they cancel each other upon summation over bonds incident to a given atom, so that the matrix of the quadratic form for the energy correction of the second order in $\delta\vec{\omega}_{bT}$, $\delta\vec{\omega}_{lT}$; T = L, R for the entire crystal has the form:

$$\begin{pmatrix} G_{bb} & H_{bb} & 0 & 0 \\ H_{bb} & G_{bb} & 0 & 0 \\ 0 & 0 & G_{ll} & H_{ll} \\ 0 & 0 & H_{ll} & G_{ll} \end{pmatrix} \quad \text{(D1)}$$

where G's and H's are proportional to the 3×3 identity matrix: $G_{bb} = g_b I$; $H_{bb} = h_b I$; $G_{ll} = g_l I$; $H_{ll} = h_l I$ (zeroes, respectively, stand for the 3×3 zero matrices), with g_b, h_b, g_l, h_l expressed through the AO–AO hopping integrals $t_{\mu\nu}$. Applying the Schur's formula for determinants,[47] we conclude that 12 eigenvalues of the above matrix have only four distinct values: $g_b \mp h_b$; $g_l \mp h_l$ each triply degenerate. Since $g_b, g_l > 0$; $g_{b,l} > h_{b,l}$, they are all positive and thus the bonding energy correction due to small rotations and deformations of the hybridization tetrahedra in the vicinity of their shapes and orientations characteristic for the lowest energy allotrope – diamond – is positive definite as well.

Acknowledgements

This paper is dedicated to Prof. Dr Karl Jug on occasion of his 80th birthday. This work is supported by the Volkswagenstiftung (grant no. 151110) "Deductive Quantum Molecular Mechanics of Carbon Allotropes" in the frame of a trilateral project between scholars and scientists from the Ukraine, Russia, and Germany. The authors are thankful to the Referees whose comments helped to improve the manuscript. Mr T. S. Kushnir (Moscow) is acknowledged for his kind help in supporting the development process and system maintenance, particularly, resolving network accessibility issues.

Notes and references

1 H. O. Pierson, *Handbook of carbon, graphite, diamond, and fullerenes: properties, processing, and applications*, Noyes Publications, 2012.
2 K. S. Novoselov, A. K. Geim, S. V. Morozov, D. Jiang, Y. Zhang, S. V. Dubonos, I. V. Grigorieva and A. A. Firsov, *Science*, 2004, **306**, 666; H. W. Kroto, J. R. Heath, S. C. O'Brien, R. F. Curl and R. E. Smalley, *Nature*, 1985, **318**, 162–163; S. Iijima and T. Ichihashi, *Nature*, 1993, **363**, 603–605.
3 Y. Yao, J. S. Tse, J. Sun, D. D. Klug, R. Martonak and T. Litaka, *Phys. Rev. Lett.*, 2009, **102**, 229601; Q. Li, Y. Ma, A. R. Oganov, H. B. Wang, H. Wang, Y. Xu, T. Cui, H. K. Mao and G. Zou, *Phys. Rev. Lett.*, 2009, **102**, 175506; Y. Liang, W. Zhang and L. Chen, *EPL*, 2009, **87**, 56003.
4 M. Hanfland, H. Beister and K. Syassen, *Phys. Rev. B: Condens. Matter Mater. Phys.*, 1989, **39**, 12598.
5 F. P. Bundy, W. A. Bassett, M. S. Weathers, R. J. Hemley, H. U. Mao and A. F. Goncharov, *Carbon*, 1996, **34**, 141.
6 F. P. Bundy and J. S. Kasper, *J. Chem. Phys.*, 1967, **46**, 3437.
7 R. T. Strong, C. J. Pickard, V. Milman, G. Thimm and B. Winkler, *Phys. Rev. B: Condens. Matter Mater. Phys.*,

2004, **70**, 045101; A. Mujica, C. J. Pickard and R. J. Needs, *Phys. Rev. B: Condens. Matter Mater. Phys.*, 2015, **91**, 214104.
8 A. R. Oganov and C. W. Glass, *J. Chem. Phys.*, 2006, **124**, 224704; Q. Li, Y. Ma, A. R. Oganov, H. Wang, H. Wang, Y. Xu, T. Cui, H.-K. Mao and G. Zou, *Phys. Rev. Lett.*, 2009, **102**, 175506; Q. Zhu, A. R. Oganov, M. A. Salvado, P. Pertierra and A. O. Lyakhov, *Phys. Rev. B: Condens. Matter Mater. Phys.*, 2011, **83**, 193410; Q. Zhu, Q. Zeng and A. R. Oganov, *Phys. Rev. B: Condens. Matter Mater. Phys.*, 2012, **85**, 201407.
9 M. Amsler, J. A. Flores-Livas, L. Lehtovaara, F. Balima, S. A. Ghasemi, D. Machon, S. Pailhes, A. Willand, D. Caliste, S. Botti, A. San Miguel, S. Goedecker and M. A. L. Marques, *Phys. Rev. Lett.*, 2012, **108**, 065501; S. Botti, M. Amsler, J. A. Flores-Livas, P. Ceria, S. Goedecker and M. A. L. Marques, *Phys. Rev. B: Condens. Matter Mater. Phys.*, 2013, **88**, 014102.
10 R. Hoffmann, A. A. Kabanov, A. A. Golov and D. M. Proserpio, *Angew. Chem., Int. Ed.*, 2016, **55**, 10962–10977.
11 P. E. Blöchl, *Phys. Rev. B: Condens. Matter Mater. Phys.*, 1994, **50**, 17953–17979; G. Kresse and D. Joubert, *Phys. Rev. B: Condens. Matter Mater. Phys.*, 1999, **59**, 1758–1775.
12 G. Kresse and J. Hafner, *Phys. Rev. B: Condens. Matter Mater. Phys.*, 1993, **47**, 558–561.
13 X. Gonze, J.-M. Beuken, R. Caracas, F. Detraux, M. Fuchs and G.-M. Rignanese, *et al.*, *Comput. Mater. Sci.*, 2002, **25**, 478–492; X. Gonze, B. Amadon, P.-M. Anglade, J.-M. Beuken, F. Bottin and P. Boulanger, *et al.*, *Comput. Phys. Commun.*, 2009, **180**, 2582–2615; X. Gonze, G.-M. Rignanese, M. Verstraete, J.-M. Beuken, Y. Pouillon and R. Caracas, *et al.*, *Z. Kristallogr. – Cryst. Mater.*, 2005, **220**, 558–562.
14 V. L. Deringer, G. Csanyi and D. M. Proserpio, *Chem. Phys. Chem.*, 2017, **18**, 1–6.
15 A. M. Tokmachev and A. L. Tchougréeff, *Int. J. Quantum Chem.*, 2002, **88**, 403–413.
16 A. L. Tchougréeff and A. M. Tokmachev, *Int. J. Quantum Chem.*, 2004, **96**, 175–184.
17 A. L. Tchougréeff and R. Dronskowski, *Mol. Phys.*, 2016, **114**, 1423–1444.
18 I. V. Popov, A. L. Görne, A. L. Tchougréeff and R. Dronskowski, *Phys. Chem. Chem. Phys.*, 2019, **21**, 10961–10969.
19 C. N. Parkinson, *Parkinson's Law (and other Studies in Administration)*, Houghton Mifflin Co, Boston, 1957.
20 R. C. Fort, Jr. and P. V. R. Schleyer, *Chem. Rev.*, 1964, **64**, 277–300.
21 X.-L. Sheng, Q.-B. Yan, F. Ye, Q.-R. Zheng and G. Su, *Phys. Rev. Lett.*, 2011, **106**, 155703.
22 A. Baeyer, *Ber. Deut. Chem. Ges.*, 1885, **18**, 2269; K. Wiberg, *Angew. Chem., Int. Ed. Engl.*, 1986, **25**, 312–322.
23 A. L. Tchougréeff, *THEOCHEM*, 2003, **630**, 243–263; A. L. Tchougréeff and A. M. Tokmachev, *Int. J. Quant. Chem.*, 2004, **96**, 175–184.
24 A. M. Tokmachev and A. L. Tchougréeff, *J. Comput. Chem.*, 2005, **26**, 491–505.
25 A. L. Tchougréeff, *J. Struct. Chem.*, 2007, **48**, S32–S54 [in English]; A. L. Tchougréeff, *Hybrid Methods of Molecular Modeling*, Springer, 2008.
26 L. Öhrström and M. O'Keeffe, *Z. Kristallogr.*, 2013, 1620.
27 C. A. Coulson, *Proc. R. Soc. London, Ser. A*, 1939, **169**, 413.
28 J. Pople and D. Beveridge, *Approximate Molecular Orbital Theory*, McGraw-Hill, 1970; I. Levine, *Quantum Chemistry*, Prentice Hall, 4th edn, 1991; C. J. Cramer, *Essentials of Computational Chemistry*, Wiley, Chichester, 2002; A. Szabo and N. S. Oslund, *Modern Quantum Chemistry: Introduction to Advanced Electronic Structure Theory*, Dover, 1996.
29 I. Mayer, *Chem. Phys. Lett.*, 1983, **97**, 270; I. Mayer, *Chem. Phys. Lett.*, 1985, **117**, 396; I. Mayer, *J. Comput. Chem.*, 2007, **28**, 204; I. Mayer, *Chem. Phys. Lett.*, 2012, **544**, 83.
30 C. C. J. Roothaan, *J. Chem. Phys.*, 1951, **19**, 1445–1458.
31 A. L. Tchougréeff, Computational Science and Its Applications – ICCSA 2019, Part IV, *Lect. Notes Comput. Sci. Eng.*, 2019, **11622**, 639–651; see also: https://cartesius.info/doxygen/ consulted 20.07.2019 (see ref. 50).
32 A. L. Görne and R. Dronskowski, *Carbon*, 2019, **148**, 151–158.
33 V. L. Deringer, A. L. Tchougréeff and R. Dronskowski, *J. Phys. Chem.*, 2011, **115**, 5461–5466; S. Maintz, V. L. Deringer, A. L. Tchougréeff and R. Dronskowski, *J. Comput. Chem.*, 2013, **34**, 2557–2567; S. Maintz, V. L. Deringer, A. L. Tchougréeff and R. Dronskowski, *J. Comput. Chem.*, 2016, **37**, 1030–1035.
34 J. M. Kennedy and C. E. Schäffer, *Inorg. Chim. Acta*, 1996, **252**, 185–194.
35 M. Esser, A. A. Esser, D. M. Proserpio and R. Dronskowski, *Carbon*, 2017, **121**, 154–162.
36 M. Hu, Y. Pan, K. Luo, J. He, D. Yu and B. Xu, *Carbon*, 2015, **91**, 518–526.
37 L. Yang, H. Y. He and B. C. Pan, *J. Chem. Phys.*, 2013, **138**, 024502.
38 H. J. McSkimin and P. Andreatch, *J. Appl. Phys.*, 1972, **43**, 2944–2948; M. H. Grimsditch and A. K. Ramdas, *Phys. Rev. B: Condens. Matter Mater. Phys.*, 1975, **11**, 3139–3148.
39 S. Shaik and P. C. Hiberty, *A Chemist's Guide to Valence Bond Theory*, John Wiley & Sons, 2007.
40 C. A. Coulson and W. E. Moffitt, *Philos. Mag.*, 1949, **40**(300), 1–35.
41 D. W. Brenner, *Phys. Rev. B: Condens. Matter Mater. Phys.*, 1990, **42**, 9458.
42 V. G. S. Box, *J. Mol. Model.*, 1997, **3**, 124–141.
43 J. Che, T. Çağın and W. A. Goddard III, *Theor. Chem. Acc.*, 1999, **102**, 346.
44 A. M. Kosevich, *Basics of the lattice mechanics (in Russian)*, Nauka, Moscow, 1972, p. 280.
45 J. F. Nye, *Physical Properties of Crystals. Their representation by tensors and matrices*, Clarendon Press, Oxford, 2006, p. 329.
46 N. I. Ostrosablin, *Sib. Zh. Ind. Mat.*, 1998, **1**, 155–163.
47 F. R. Gantmacher, *The theory of matrices*, Chelsea Pub. Co., 1960.
48 M. D. Foster, M. M. J. Treacy, J. B. Higgins, I. Rivin, E. Balkovsky and K. H. Randall, *J. Appl. Crystallogr.*, 2005, **38**, 1028–1030, http://www.hypotheticalzeolites.net/NEWDATABASE/search.php consulted on 20 July 2019.
49 I. A. Baburin, D. M. Proserpio, V. A. Saleev and A. V. Shipilova, *Phys. Chem. Chem. Phys.*, 2015, **17**, 1332–1338.
50 NetLaboratory at https://netlab.cartesius.info; this is a perfectly safe website without any malicious code despite erroneous warnings by some antivirus software packages; for more information, please check our root certificates at https://www.ssllabs.com/ssltest/analyze.html?d=cartesius.info.

